

Physical and Chemical Properties of Nanocomposite Polymer Electrolytes

F. Croce, R. Curini, A. Martinelli, L. Persi, F. Ronci, and B. Scrosati*

Dipartimento di Chimica, Università "La Sapienza", 00185 Rome, Italy

R. Caminiti

Istituto Nazionale di Fisica della Materia (INFM), Italy

Received: July 7, 1999; In Final Form: September 13, 1999

The physical and chemical properties of a new class of lithium conducting polymer electrolytes formed by dispersing ceramic powders at the nanoscale particle size into a poly(ethylenoxide) (PEO)–lithium salt, LiX complexes, are reported and discussed. These true solid-state PEO–LiX nanocomposite polymer electrolytes have in the 30–80 °C range an excellent mechanical stability (due to the network of the ceramic fillers into the polymer bulk) and high ionic conductivity (promoted by the high surface area of the dispersed fillers). These important and unique properties are accompanied by a wide electrochemical stability and by a good compatibility with the lithium electrode (assured by the absence of any liquids and by the interfacial stabilizing action of the dispersed filler), all this making these nanocomposite electrolytes of definite interest for the development of advanced rechargeable lithium batteries.

Introduction

A polymer electrolyte may be generally defined as a membrane having transport properties comparable with those of the common liquid ionic solutions. Classical examples are membranes formed by complexes between a lithium salt, LiX, e.g., LiClO₄ or LiN(CF₃SO₂)₂, and a high molecular weight polymer containing Li⁺-coordinating groups, e.g., poly(ethylene oxide), PEO. The basic structure of these membranes involves PEO chains coiled around the Li⁺ cations, this separating them from the X⁻ counteranions.¹ This favors the dissolution of the LiX salt in the PEO matrix with a solvating mechanism which is in effect similar to that occurring in the liquid electrolytes. However, due to their particular configuration, polymer electrolytes require local relaxation and segmental motion of the solvent (i.e., PEO) chains to allow ion (i.e., Li⁺) transport, and this condition can only be obtained when the polymer is in its amorphous state. Because of the tendency of the PEO to crystallize below 70 °C, the conductivity of PEO–LiX polymer electrolytes reaches practically useful values (i.e., of the order of 10⁻⁴ S cm⁻¹) only at temperatures above this and typically, around 90 °C.²

Large research efforts have been devoted to lower to the ambient region the temperature of operation of the PEO–LiX polymer electrolytes. The most common approach has been that of adding liquid plasticizers, e.g., low molecular weight polyethylene glycols or aprotic organic solvents, to the PEO–LiX matrix. However, the addition of liquids results in a deterioration of the electrolyte's mechanical properties and greatly increases its reactivity toward the lithium metal anode.^{3,4} Therefore, the gain in conductivity is adversely accompanied by a loss of the solid-state configuration and by a loss of the compatibility with the lithium electrode, i.e., by a loss of the most important intrinsic features of the polymer electrolyte. This reflects in the fact that liquid plasticizer-added PEO–LiX electrolytes cannot be used in lithium metal batteries since

affected by a limited processability and by high reactivity with the metal anode, both drawbacks resulting in serious problems in terms of battery cyclability and safety hazards. Indeed, only dry (i.e., liquid plasticizer-free) polymer electrolytes can ensure an efficient cyclability of the lithium metal electrode, as clearly confirmed by recent papers.^{5,6}

On the other hand, this enhancement in interfacial stability has been so far adversely accompanied by a decay in room temperature conductivity, since dry electrolytes conduct only above 70 °C. Therefore, the ideal achievement in electrolytes of the PEO–LiX type is the enhancement of low-temperature ionic conductivity by modifications which avoid any liquid contamination. This goal is not easily achievable since fast ion transport in PEO–LiX is a characteristic of the amorphous state which is intrinsically reached above 70 °C or artificially induced at lower temperature by the addition of liquid plasticizers. We have proposed a novel approach based on the addition of "solid plasticizers", in the form of ceramic powders at the nanoscale particle size.⁷ The idea is to develop true solid-state PEO–LiX composite polymer electrolytes having in the 30–80 °C range excellent mechanical stability (promoted by the network of the fillers into the polymer bulk) and high ionic conductivity (induced by the high surface area of the dispersed fillers).

The general concept of adding ceramic powders to PEO–LiX polymer electrolytes is not new. In the past, this procedure has been successfully employed for improving the mechanical⁸ and the interfacial^{9–15} properties of the PEO–LiX electrolytes. However, to our knowledge, this procedure has never been used for promoting low-temperature conductivity. The innovation here proposed is based on the selection of ceramics having proper nanoscale dimensions and suitable surface characteristics and it derives from earlier results obtained in our laboratory combined with information obtained from literature work. Indeed, observations of a certain conductivity enhancement following the addition of ceramic powders were reported in the past by us¹⁶ and by others,^{17–21} albeit the ceramic filler's effective role in promoting the ion transport was never clearly

* To whom correspondence should be addressed. E-mail: scrosati@uniroma1.it.

identified. In the early 1990s, Raman spectroscopy studies had suggested that the structural properties of solid composite PEO–LiX electrolytes contained dispersed, low particle size ceramic fillers (e.g., γ -LiAlO₂ fillers) could be comparable with those of liquid electrolytes formed by low molecular weight polyethylene glycol–lithium salt solutions.¹⁶ More recently, Peled and co-workers¹⁷ reported by ⁷LiNMR studies that the addition of nanoparticle size Al₂O₃ to concentrated PEO–LiI polymer electrolytes suppresses the formation of crystalline phases. Similarly, Wieczorek et al.^{19,20} have reported that a reduction below 4 μ m of the particle size of added Al₂O₃ ceramics in composite PEO–NaI electrolytes is accompanied by a consistent increase of ionic conductivity. These authors also suggested an active role of the surface groups of the ceramic particles in promoting local structural modifications. Finally, recent work obtained at the University of Pavia demonstrated that the addition of nanoscale SiO₂ filler to the PEO–LiN(CF₃SO₂)₂ systems induces an increase in conductivity of more than 1 order of magnitude.²²

A careful examination of these literature works leads to the conclusion that the dispersed ceramics influence the recrystallization kinetics of the PEO polymer chains, this ultimately promoting local amorphicity and, thus, enhancement of the Li⁺ ion transport. Therefore, one can consider to tailor these structural modifications by selecting inorganic fillers having appropriate chemical and morphological properties. To test this concept, we have developed composite polymer electrolytes formed by dispersing into a PEO–LiClO₄ matrix titania and alumina-based, respectively, ceramic powders with particle size reduced to the nanoscale region.

Preliminary results have demonstrated the validity of this approach,^{7,23} and in this paper we confirm it by reporting a detailed study of the physical and chemical properties of this new class of “nanocomposite polymer electrolytes”.

Experimental Section

For the preparation of nanocomposite polymer electrolytes, we have selected high molecular weight poly(ethylene oxide), PEO, as the preferred polymer component, lithium perchlorate, LiClO₄, as the preferred LiX lithium salt, and TiO₂ and Al₂O₃, respectively, as the suitable ceramic filler. The LiClO₄/PEO ratio was fixed to one-eighth concentration, and the amount of added ceramic was fixed to 10% of the total PEO₈LiClO₄ weight. The TiO₂ 13 nm particle size (Degussa, and CISE²⁴) and the Al₂O₃, 5.8 nm particle size (Aldrich) ceramic fillers were dried at 250 °C for 16 h before use. Poly(ethylene oxide), PEO, a 4 000 000 MW, DBH product was purified by heating under vacuum at 50 °C. The preparation of the nanocomposite electrolyte samples involved first the dispersion of the selected ceramic powder and of the LiClO₄ lithium salt in acetonitrile, followed by the addition of the PEO polymer component and by a thorough mixing of the resulting slurry. The slurry was then cast on a Teflon plate. The procedures yielded homogeneous and mechanically stable membranes of average thickness of 100 μ m. The same casting procedure was also used for to prepare ceramic-free PEO–LiClO₄ samples used for comparison purpose.

The infrared spectra were obtained at ambient temperature with 8 cm⁻¹ resolution. The differential scanning calorimetry measurements were performed at a rate of 10 °C min⁻¹ in the 25–110 °C temperature range. The structural studies were performed by using an energy-dispersive X-ray diffractometer (EDXD) with the technique described in ref 25 to which we refer the interested reader. The diffraction measurements were

performed in the transmission geometry, fixing the scattering angle at 3.5°. In this way, we explored a range of reciprocal space of 0.6–2.8 Å⁻¹, as can be seen in Figure 7. This range contains all the interesting features of polymer diffractograms, that is to say all the typical low q peaks. The working conditions of the X-ray source were 45 kV of high voltage supply and 35 mA of cathode current. The spectra were collected for 1000 s each.

The stress–strain determination was achieved using an INSTRON 4502 instrumentation. The measurements were carried out in air at a stress velocity of 500 mm min⁻¹.

The ionic conductivity of the membrane was determined by measuring at various temperatures and in the 1 Hz to 65 kHz frequency range, the impedance of cells formed by sandwiching the given electrolyte sample between two polished stainless steel electrodes. A Solartron model 1260 frequency response analyzer was used for running this test. The conductivity results are reported in the form of Arrhenius plots determined during both heating and cooling scans.

The lithium transference number, T_{Li}^+ , was evaluated using the method originally proposed by Vincent and co-workers²⁶ and later refined by Abraham and co-workers.²⁷ According to this method, the T_{Li}^+ values have been determined by imposing a dc polarization pulse to a cell of the Li/electrolyte sample/Li type and by following the time evolution of the resulting current flow. The purpose is to measure the initial (I_0) and the steady-state (I_{ss}) values of the current flowing through the cell during polarization. Impedance spectra were taken before and after the pulse application in order to correct for the changes in impedance of the test cell during the experiment. Furthermore, we have developed special software capable of acquiring up to 5000 current data per second during the initial part of the polarization in order to be able to improve the accuracy of the extrapolated I_0 value.

The electrochemical stability window of the nanocomposite polymer electrolytes has been evaluated by running a linear sweep voltammetry of cells using a “blocking”, e.g., nickel electrode, a lithium counter, a lithium reference electrode, and the given nanocomposite sample as electrolyte. The irreversible onset of the current on the anodic region is assumed as the electrolyte breakdown voltage.

The lithium electrode–polymer electrolyte interfacial phenomena have been evaluated by monitoring the impedance response of cells again formed by sandwiching the given electrolyte sample between two lithium electrodes. The cells were stored under open circuit conditions, and their impedance response was analyzed using the fitting program proposed by Boukamp.²⁸ This procedure allowed separation of the contributions of the various phenomena which concur to determine the interfacial resistance.

Results and Discussion

Figure 1 shows the conductivity Arrhenius plots of a representative example of these nanocomposite polymer electrolytes, i.e., the PEO₈LiClO₄.10 w/o Al₂O₃ sample. Also, the plot of a ceramic-free PEO₈LiClO₄ polymer electrolyte is reported for comparison purposes. The heating scan of the latter shows a break around 70 °C, reflecting the well-known transition from the PEO crystalline to the amorphous state, which is accompanied by a relevant increase in ionic conductivity. When brought back below 70 °C, the common PEO₈LiClO₄ electrolyte initially remains in the amorphous state due to the rather slow recrystallization kinetics. However, this electrolyte tends to readily recrystallize and, consequently, its conductivity to decay.

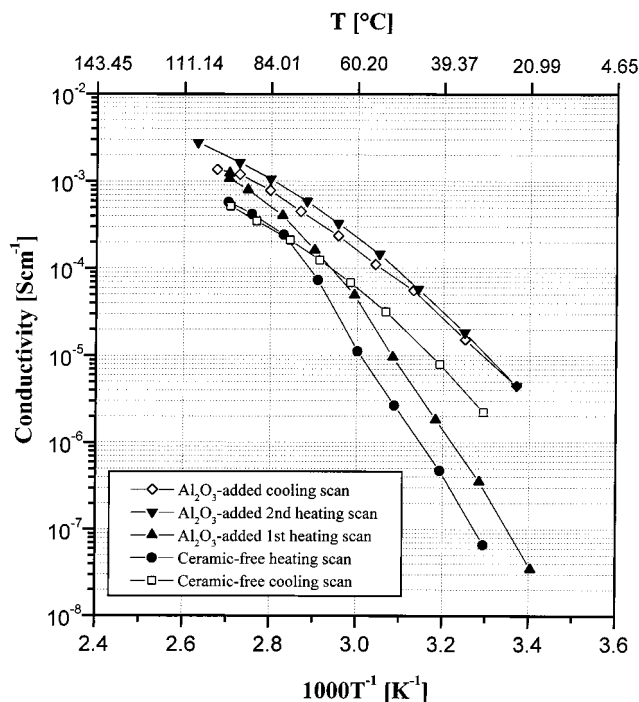


Figure 1. Arrhenius plots of the conductivity of ceramic-free $\text{PEO}_8\text{-LiClO}_4$ and of the nanocomposite $\text{PEO}_8\text{-LiClO}_4.10$ w/o Al_2O_3 polymer electrolyte. Data obtained by impedance spectroscopy measurements.

The as-prepared nanocomposite electrolyte has a room temperature conductivity and a first heating scan similar to that of the plain electrolyte. However, the behavior of the following cooling scan is quite different since no break occurs around 70°C and the conductivity remains consistently higher, i.e., comprised between 10^{-3} and 10^{-5} S cm^{-1} versus 10^{-4} and 10^{-8} S cm^{-1} in the $80\text{--}30^\circ\text{C}$ temperature range. This conductivity trend is reproduced in the following heating and cooling scans. A similar behavior is also displayed by the $\text{PEO}_8\text{-LiClO}_4.10$ w/o TiO_2 nanocomposite polymer electrolyte, as shown by the related Arrhenius plot reported in Figure 2. This enhancement in conductivity is quite stable, as demonstrated by Figure 3 which shows the time evolution of the room-temperature conductivity of the $\text{PEO}_8\text{-LiClO}_4.10$ w/o TiO_2 electrolyte.

Our first concern was to verify that the observed enhancement in conductivity was effectively due to the action of the nanoceramic filler and not to some side effects, such as excess of residual casting solvent. Parts A and B of Figure 4 show the IR spectra for the TiO_2 -based and the Al_2O_3 -based, respectively, nanocomposite polymers. For both samples, the small band around 2500 cm^{-1} related to the $\text{-C}\equiv\text{N}$ stretching is good evidence that the trace content of residual acetonitrile casting solvent is negligible in both electrolytes. This rules out the chance that the conductivity enhancement in the nanocomposite electrolytes, rather than being due to a faster ion transport, could have been related to a dilution and/or plasticizing effect promoted by an excess of liquid adsorbed by the ceramics during casting and released in the electrolyte bulk during the heating scan. In addition, stress-strain measurements revealed a large enhancement of the Young's modulus and of the yield point stress when passing from ceramic-free to nanocomposite polymer electrolyte samples, this demonstrating that the conductivity state of the latter is not due to polymer degradation but rather is accompanied by a substantial increase in the electrolyte's mechanical properties.

It is then reasonable to conclude that the favorable transport behavior is an inherent feature of the nanocomposite structure.

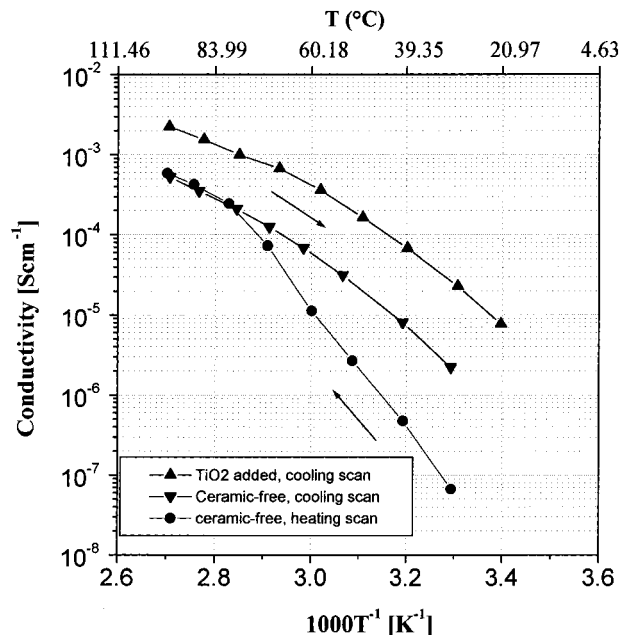


Figure 2. Arrhenius plots of the conductivity of the nanocomposite $\text{PEO}_8\text{-LiClO}_4.10$ w/o TiO_2 polymer electrolyte. Data obtained by impedance spectroscopy measurements.

A possible explanation of this behavior is that, once the composite electrolytes are annealed at temperatures higher than the PEO crystalline to amorphous transition (i.e., above 70°C), the ceramic additive, due to its large surface area, prevents local PEO chain reorganization with the result of freezing at ambient temperature a high degree of disorder which is likely to be accompanied by a consistent enhancement of the ionic conductivity.

Accordingly, one may assume that the structural modification is induced via Lewis acid-base reactions between the ceramic surface states and the PEO segments, as indeed already proposed by Wiczcerek et al.^{19,20} The Lewis acid character of the added ceramics would compete with the Lewis acid character of the lithium cations for the formation of complexes with the PEO chains. Thus, the ceramics would act as cross-linking centers for the PEO segments, this lowering the polymer chain reorganization tendency and promoting an overall structure stiffness. Such a structure modification would provide Li^+ conducting pathways at the ceramics' surface, this accounting for the improvement in ionic transport.

We have undertaken a series of complementary tests to support the conductivity data and the postulated transport mechanism. In this respect we have measured the lithium ion transference number T_{Li^+} of the two types of nanocomposite electrolytes. It has first to be pointed out that in conventional, ceramic-free PEO-LiX electrolytes, the fraction of current transported by the Li^+ cations is lower than that of the X^- anions and, thus, T_{Li^+} is usually in the 0.2 range.² This is a consequence of the structural position of the Li^+ cations which sit within a coiled PEO chains coordinating environment. In contrast to the relatively free movement of the uncoordinated anions, the movement of these cations requires relaxation and segmental motion of the chains and this explains their lower mobility. The second aspect to be remarked is that ion transference measurements are not easy in polymer electrolytes since complicated by various side phenomena.²⁶ For the nanocomposite polymer electrolytes discussed in this work, we have used the most recommended techniques which basically require to impose dc voltage pulses to cells of the $\text{Li}/\text{electrolyte sample}/\text{Li}$ type and

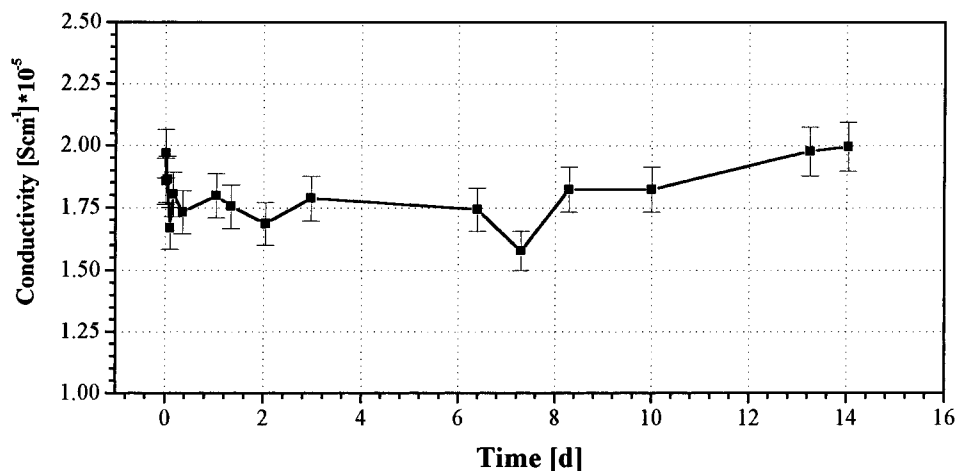


Figure 3. Changes upon time of the conductivity of nanocomposite PEO₈LiClO₄.10 w/o TiO₂ polymer electrolyte at room temperature. Data obtained by impedance spectroscopy measurements.

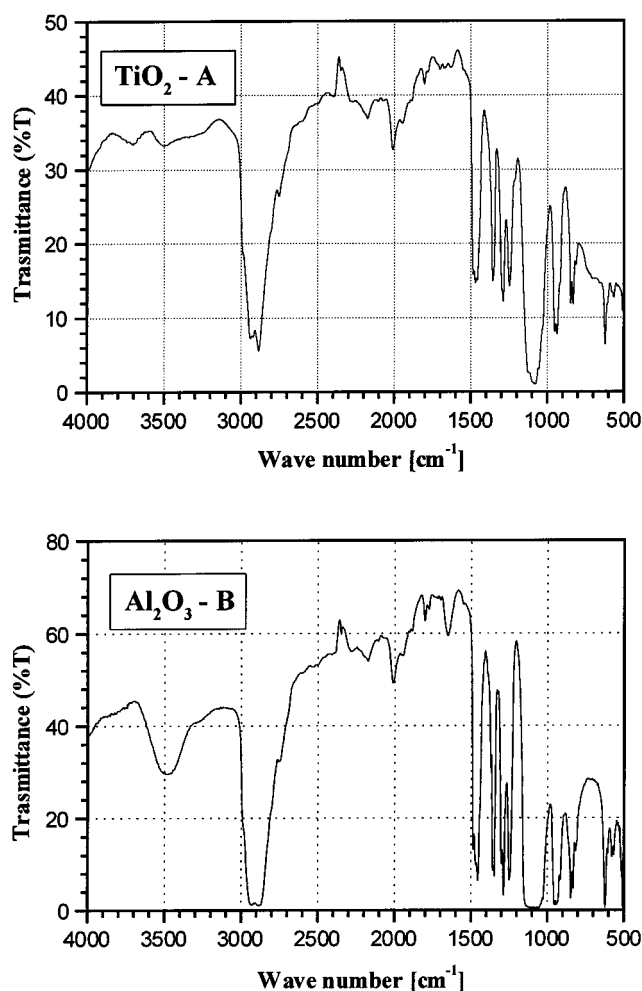


Figure 4. IR spectra of PEO₈LiClO₄.10 w/o TiO₂ (A) and PEO₈LiClO₄.10 w/o Al₂O₃ (B) nanocomposite polymer electrolytes.

to follow the time evolution of the resulting current flow. The accuracy of this technique may be affected by the difficulty of detecting the evolution of the current values immediately after the application of the voltage polarization pulse. To solve this problem, we have developed a special acquisition program which has allowed us to store data at very short time intervals. Figure 5 shows a typical current–time data acquisition plot related to the PEO₈LiClO₄.10 w/o TiO₂ case. The T_{Li^+} values obtained with this refined technique are reported in Table 1.

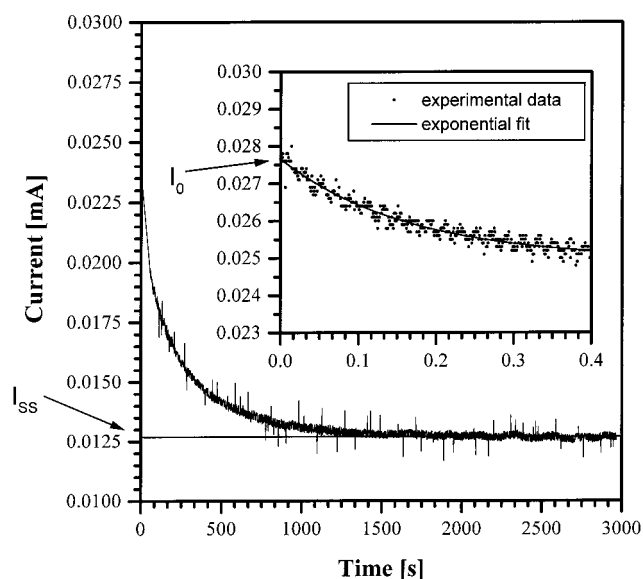


Figure 5. Current–time curve of a Li/PEO₈LiClO₄.10 w/o TiO₂/Li cell following the application of a 10 mV polarization pulse up to steady-state conditions for the determination of I_{ss} . The inset shows the current values acquisition during the first few tenths of second after pulse application for the determination of I_0 .

TABLE 1: Lithium Transference Number for the PEO₈LiClO₄.10 w/o Ceramic Added Nanocomposite Polymer Electrolytes at 91 °C

ceramic	T_{Li^+}
free	0.25
TiO ₂	0.5–0.6
Al ₂ O ₃	0.3

The results are consistent in demonstrating a difference in T_{Li^+} in passing from the ceramic-free to the nanocomposite polymer electrolytes. In addition, the T_{Li^+} values consistently vary according to the Lewis acid character of the added ceramic. For the most acidic type, i.e., the TiO₂ one, the transference number value increases up 0.5–0.6 in the 45–90 °C temperature range. To our knowledge, such a high value has never been reported for common PEO-based electrolytes. This value, however, is consistent with the transport model above proposed, according to which the action of the ceramic filler is that of promoting surface conducting pathways as a result of its Lewis acid type interactions with the PEO chains. Lithium ions are expected to move freely along these ceramic surface pathways

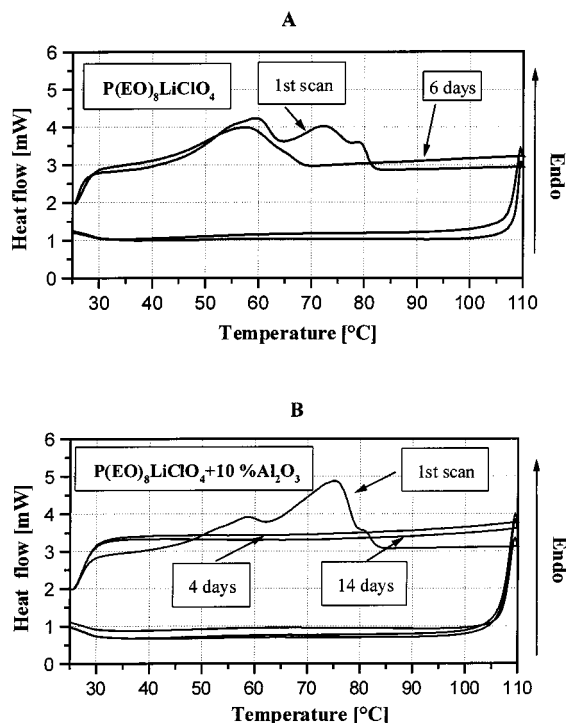


Figure 6. DSC traces of ceramic-free $\text{PEO}_8\text{LiClO}_4$ (A) and of $\text{PEO}_8\text{LiClO}_4.10$ w/o TiO_2 nanocomposite (B) polymer electrolyte samples. The traces refer to the first heating–cooling scan of as-prepared samples and to heating–cooling scans after a different number of days of storage at room temperature. Heating–cooling rate: $10^\circ\text{C min}^{-1}$.

and thus, under these conditions, a consistent enhancement of the cation transference number is logically expected. It is interesting to report that Magistris et al. have also found that the addition of nanometric silica to a $\text{PEO}_8\text{LiClO}_4$ polymer causes the lithium transport number to nearly redouble.²²

Figure 6 shows differential scanning calorimetry, DSC, traces of ceramic-free $\text{PEO}_8\text{LiClO}_4$ (A) and of $\text{PEO}_8\text{LiClO}_4.10$ w/o Al_2O_3 nanocomposite (B) polymer electrolyte samples. In both cases, traces referring to the first heating–cooling scan of as-prepared samples and to heating–cooling scans run after a different number of days of storage at room temperature are shown. Let us first consider the response of the ceramic-free sample. The first heating scan shows the expected crystalline to amorphous peak at $60\text{--}70^\circ\text{C}$ and the immediately following cooling scan from 100°C to room temperature is peakless, since even the ceramic-free electrolytes have a relatively slow recrystallization kinetics.²⁹ However, this electrolyte does recrystallize, as indeed shown by the peak of the trace obtained after 6 days of storage at room temperature. Quite different is the DSC response for the Al_2O_3 -added composite electrolyte, Figure 6B. As expected and in agreement with the conductivity results (Figure 1), a peak due to the crystalline to amorphous transition is shown around $60\text{--}70^\circ\text{C}$ in the first heating scan. However, in all following heating and cooling scans, no peaks are revealed even after prolonged storage times (i.e., exceeding 2 weeks), this again confirming the conductivity results (Figure 3) and, ultimately, that after being annealed at temperatures above the PEO transition, the nanocomposite polymer electrolytes retain their amorphous state even if kept at room temperature for many days. This result also confirms the crucial role of the added nanoceramics in influencing the recrystallization kinetics of PEO–LiX polymer electrolytes.

This important and unique role of the nanoceramic additive was further analyzed by the energy dispersive X-ray diffraction

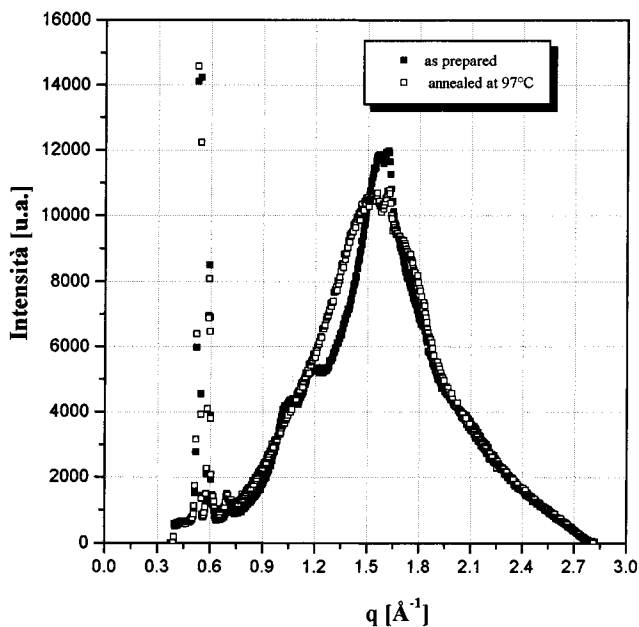


Figure 7. Energy dispersive X-ray diffraction analysis of an as-prepared nanocomposite $\text{PEO}_8\text{LiClO}_4.10$ w/o TiO_2 sample and of the same sample after annealing at 97°C .

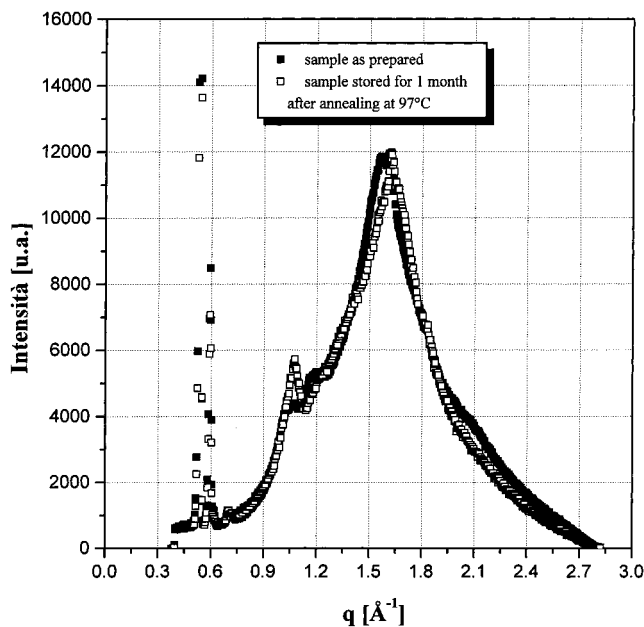


Figure 8. Energy dispersive X-ray diffraction analysis of an as-prepared nanocomposite $\text{PEO}_8\text{LiClO}_4.10$ w/o TiO_2 sample and of the same sample stored for 31 days after annealing at 97°C .

(EDXD) technique. The validity of this unconventional diffractometric technique for investigating the crystallization kinetics in polymers has been outlined in a previous paper.²⁹ Figure 7 shows in comparison the spectrum obtained on an as-prepared $\text{PEO}_8\text{LiClO}_4.10$ w/o TiO_2 nanocomposite electrolyte sample and that of the same sample after annealing at 97°C . Supporting the above-discussed transport and thermal data, the crystalline feature observed in the pristine state disappears after annealing.

A key question is whether the annealed nanocomposite sample may eventually recrystallize as well. To answer to this question, we have monitored the time evolution of the EDXD spectra of an annealed $\text{PEO}_8\text{LiClO}_4.10$ w/o TiO_2 sample. The sample was continuously kept under the X-ray control. Figure 8 compares the spectrum of an as-prepared sample with that of the same sample stored at room temperature for 1 month after annealing

Linear sweep voltammetry on Li/PEO₈LiClO₄+10% TiO₂/Ni cell
T = 90°C, v = 0.1 mV/s

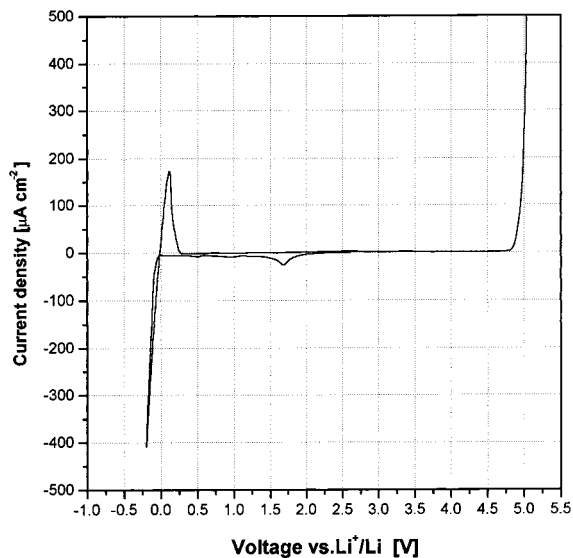


Figure 9. Cyclic voltammety of a nickel electrode in a nanocomposite PEO₈LiClO₄. 10 w/o TiO₂ polymer electrolyte cell. Lithium counter and lithium reference electrode: scan rate, 0.2 mV s⁻¹; temperature, 90 °C; electrode area, 1.13 cm².

at 97 °C. The result shows that indeed after prolonged storage some recrystallization does occur. However, the feature of the recrystallized sample spectrum is different from that of the as-prepared sample. This drives to an important conclusion, namely that the nanocrystalline samples recrystallize by assuming a structure which is somewhat different from that of common PEO–LiX polymer electrolytes. This phenomenon, to our knowledge never so far observed, confirms the postulated role of the nanoceramic filler in establishing interactions with the PEO chains which ultimately may lead to changes in the electrolyte microstructure. This is further supported by the fact that we have observed that the recrystallization kinetics appear to be critically depending upon annealing conditions, e.g., time and temperature. This model is supported by the results here presented which allow to conclude that the addition of ceramic fillers of proper chemical nature and particle size may effectively enhance the transport properties of PEO–LiX polymer electrolytes without affecting but rather enforcing their mechanical properties. This is an important property in view of the most probable applications of these materials, i.e., as electrolyte separators in lithium batteries. Since ideally based on a lithium metal anode and a lithium-intercalating cathode,^{30,31} these batteries may greatly benefit by a solid polymer electrolyte with appreciable ambient temperature conductivity and high lithium ion transference number.

However, in view of this type of application, a high conductivity is not a sufficient property to make an electrolyte useful in practical terms. Also wide electrochemical stability and compatibility with the lithium metal electrode are essential parameters for ensuring good performance in rechargeable lithium batteries. The electrochemical stability window of the nanocomposite polymer electrolytes has been evaluated by running a cyclic voltammety of cells using a “blocking”, e.g., nickel electrode, a lithium counter, and a lithium reference electrode. Figure 9 shows typical results obtained on a cell using a PEO₈LiClO₄.10 w/o TiO₂ nanocomposite electrolyte sample. The irreversible onset of the current on the anodic region determines the electrolyte breakdown voltage, which in the case

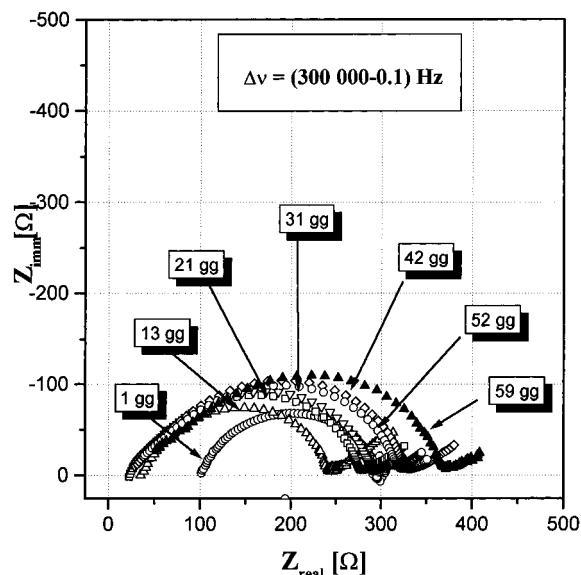


Figure 10. Impedance spectra of a Li/PEO₈LiClO₄.10 w/o Al₂O₃/Li cell as a function of storage time at 91 °C. Frequency range: 10 mHz to 150 kHz.

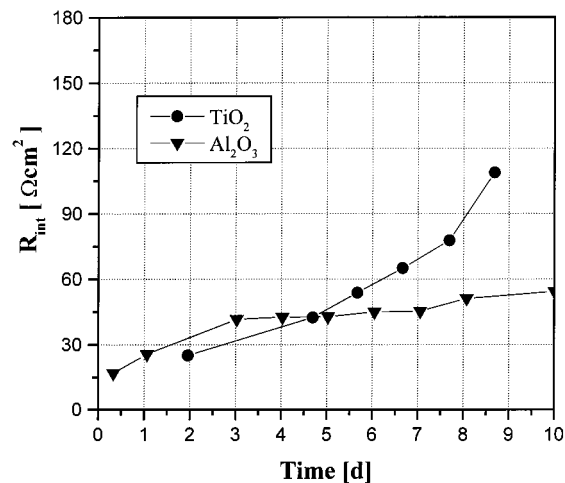


Figure 11. Change of interfacial resistance R_i in Li/PEO₈LiClO₄+10 w/o nanoceramic additive/Li cells at 91 °C.

of Figure 9 extends to about 5 V vs Li. The cathodic peak at the other extreme, i.e., at about 0 V vs Li corresponds to the lithium deposition on the nickel substrate and is reproduced by a peak in the reverse scan which corresponds to the stripping of lithium. This lithium deposition-stripping process is reversible, since the integrated charges in the cathodic and anodic peaks are comparable. A similar behavior has been found with cells using the Al₂O₃-based nanocomposite electrolyte. The voltammetric results, beside providing evidence of a high anodic stability of these electrolytes, also suggest their good compatibility with the lithium metal electrode. The latter aspect has been further examined with an impedance investigation of the lithium electrode/nanocomposite polymer electrolyte interfacial properties. This has been accomplished by monitoring the time evolution of impedance response of Li/nanocomposite polymer electrolyte/Li cells under open circuit potential at 91 °C. Figure 10 shows the results in terms of imaginary $-jZ''$ versus real Z' plots for a cell using the Al₂O₃-based electrolyte. Similar plots have been obtained with TiO₂-based cells. By using a proper fitting program,²⁸ it was possible to determine from the low-frequency intercept on the real axis the time evolution of the lithium interfacial resistance R_i , as reported in Figure 11. This resistance,

which may be associated with the formation and the growth of a passivation layer on the lithium electrode surface,³ does not change consistently with time and, particularly in the case of the Al₂O₃-based electrolyte, remains at a low value under a prolonged time scale. This high stability, probably assured by the absence of any liquids and by the interfacial stabilizing action of the dispersed filler,^{5,6} is a convincing evidence that the lithium passivation in the nanocomposite electrolytes is a controlled phenomenon and thus, that these electrolytes have a sufficient compatibility with the lithium electrode to allow safe operation in rechargeable lithium batteries. Further investigation is in progress to confirm this important expectation.

Acknowledgment. This work has been carried out with financial support provided by ENEA, Contract 1221 and by the U.S. Army European Research Office (Contract N 68171-99-M-6040).

References and Notes

- (1) Lightfoot, P.; Metha, M. A.; Bruce, P. G. *Science* **1993**, *262*, 883.
- (2) Gray, F. M. *Solid Polymer Electrolytes-Fundamentals and Technical Applications*; VCH: Weinheim, Germany, 1991.
- (3) Croce, F.; Scrosati, B. *J. Power Sources* **1993**, *43*, 43.
- (4) Scrosati, B. *Chim. Ind. (Milan)* **1995**, *77* (5), 285.
- (5) Appetecchi, G. B.; Croce, F.; Dautzenberg, G.; Mastragostino, M.; Ronc, F.; Scrosati, B.; Soavi, F.; Zanelli, F.; Alessandrini, F.; Prosini, P. P. *J. Electrochem. Soc.* **1998**, *145*, 4126.
- (6) Appetecchi, G. B.; Croce, F.; Mastragostino, M.; Scrosati, B.; Soavi, F.; Zanelli, F. *J. Electrochem. Soc.* **1998**, *145*, 4133.
- (7) Croce, F.; Appetecchi, G. B.; Persi, L.; Scrosati, B. *Nature* **1998**, *394*, 456.
- (8) Weston, J. E.; Steele, B. C. H. *Solid State Ionics* **1982**, *7*, 75.
- (9) Scrosati, B. *J. Electrochem. Soc.* **1990**, *136*, 2774.
- (10) Croce, F.; Scrosati, B. *J. Power Sources* **1993**, *43*, 43.
- (11) Borghini, M. C.; Mastragostino, M.; Passerini, S.; Scrosati, B. *J. Electrochem. Soc.* **1995**, *142*, 2118.
- (12) Capuano, F.; Croce, F.; Scrosati, B. U.S. Patent 5,576,115, Nov. 19, 1996.
- (13) Peled, E.; Golodnitsky, D.; Ardel, G.; Eshkenazy, V. *Electrochim. Acta* **1995**, *40*, 2197.
- (14) Kumar, B.; Scanlon, L. G. *J. Power Sources* **1994**, *52*, 261.
- (15) Quartarone, E.; Mustarelli, P.; Magistris, A. *Solid State Ionics* **1998**, *110*, 1.
- (16) Croce, F.; Scrosati, B. *Philos. Mag. B* **1988**, *59*, 151. Croce, F.; Scrosati, B. *Polym. Adv. Technol.* **1993**, *4*, 198. Capuano, F.; Croce, F.; Scrosati, B. *J. Electrochem. Soc.* **1991**, *138*, 1918.
- (17) Dai, Y.; Greenbaum, S.; Golodnitsky, D.; Ardel, G.; Strauss, E.; Peled, E.; Rosenberg, Yu. *Solid State Ionics* **1988**, *106*, 25.
- (18) Croce, F.; Scrosati, B.; Mariotto, G. *Chem. Mater.* **1992**, *4*, 1134.
- (19) Wiczorek, W.; Florjanczyk, Z.; Stevens, J. R. *Electrochim. Acta* **1995**, *40*, 2251.
- (20) Przyluski, J.; Siekierski, M.; Wiczorek, W. *Electrochim. Acta* **1995**, *40*, 2101.
- (21) Krawiec, W.; Scanlon, L. G.; Fellner, J. P.; Vaia, R. A.; Vasudevan, S.; Giannelis, E. P. *J. Power Sources* **1995**, *54*, 310.
- (22) Capiglia, C.; Mustarelli, P.; Quartarone, E.; Tomasi, C.; Magistris, A. *Solid State Ionics*, in press.
- (23) Croce, F.; Appetecchi, G. B.; Persi, L.; Scrosati, B. *Solid State Ionics*, in press.
- (24) Thanks are expressed to Dr. Musci M. of the CISE Laboratory, Milan, for having kindly provided samples of TiO₂ nanopowders.
- (25) Rossi Albertini, V.; Bencivenni, L.; Caminiti, R.; Cilloco, F.; Sadun, C. *J. Macromol. Sci. Phys.* **1996**, *B35*, 19. Rossi Albertini, V.; Caminiti, R.; Cilloco, F.; Croce, F.; Sadun, C. *J. Macromol. Sci. Phys.* **1997**, *B36* (2), 221. Caminiti, R.; Rossi Albertini, V. *Int. Rev. Phys. Chem.* **1999**, *18* (2).
- (26) Evans, J.; Vincent, C. A.; Bruce, P. G. *Polymer* **1987**, *28*, 2325.
- (27) Abraham, K. M.; Jiang, Z.; Carroll, B. *Chem. Mater.* **1997**, *9*, 1918.
- (28) Boukamp, A. *Solid State Ionics* **1986**, *20*, 31.
- (29) Rossi Albertini, V.; Appetecchi, G. B.; Caminiti, R.; Cilloco, F.; Croce, F.; Sadun, C. *J. Macromol. Sci.* **1997**, *B36* (2), 629.
- (30) Vincent, C. A.; Scrosati, B. *Modern Batteries. An Introduction to Electrochemical Power Sources*, 2nd ed.; Arnold: London, 1997.
- (31) Scrosati, B. *Chim. Ind. (Milan)* **1997**, *79*, 463.